



Deposited via The University of Leeds.

White Rose Research Online URL for this paper:

<https://eprints.whiterose.ac.uk/id/eprint/160366/>

Version: Accepted Version

Article:

Livermore, PW, Finlay, CC and Bayliff, M (2020) Recent north magnetic pole acceleration towards Siberia caused by flux lobe elongation. *Nature Geoscience*, 13 (5). pp. 387-391. ISSN: 1752-0894

<https://doi.org/10.1038/s41561-020-0570-9>

This item is protected by copyright, all rights reserved. This is an author produced version of an article published in *Nature Geoscience*. Uploaded in accordance with the publisher's self-archiving policy.

Reuse

Items deposited in White Rose Research Online are protected by copyright, with all rights reserved unless indicated otherwise. They may be downloaded and/or printed for private study, or other acts as permitted by national copyright laws. The publisher or other rights holders may allow further reproduction and re-use of the full text version. This is indicated by the licence information on the White Rose Research Online record for the item.

Takedown

If you consider content in White Rose Research Online to be in breach of UK law, please notify us by emailing eprints@whiterose.ac.uk including the URL of the record and the reason for the withdrawal request.

25 location where the horizontal component of magnetic field H was zero and a mag-
26 netic needle pointed directly down to the center of the Earth [3]. Such direct deter-
27 minations are difficult, especially if the pole position is not on land and because of
28 field fluctuations due to currents in the high latitude ionosphere [4]. More recently
29 the magnetic pole position has been determined from global models of the geo-
30 magnetic field [5] built using measurements made by both satellites and by a net-
31 work of ground observatories. The accuracy of such pole determinations, which
32 depends on the quality and distribution of the contributing observations along with
33 the ability to remove the external magnetic field, has steadily improved over time;
34 since 1999 there has been continuous monitoring of the geomagnetic field from
35 space by a series of dedicated satellite missions, most recently the Swarm mission
36 [6]. In Fig 1 we show the path of the pole since 1840 from the COV-OBS.x1
37 [7] and CHAOS-6-x8 [8] geomagnetic field models alongside in-situ historical
38 measurements. The location of the magnetic pole is a characteristic of the core-
39 generated magnetic field that is spherically-radially attenuated through the mantle,
40 which may be considered as an electrical insulator on the time-scales of relevance
41 here. The magnetic pole's position is thus only an indirect indicator of the state of
42 Earth's dynamo. However the specific geometry of the magnetic field on Earth's
43 surface is of broad societal importance, as was demonstrated recently by the need
44 for a high-profile irregular update in 2019 of the world magnetic model used for
45 navigation in many mobile devices [9].

46 **Recent movement of the north magnetic pole**

47 Compared with its meandering position prior to the 1970s, over the past 50 years
48 the north magnetic pole has travelled along a remarkably linear path that is un-
49 precedented in the recent historical record [10; 11; 12], guided along a trough of
50 low horizontal field [10; 13]. Using high-resolution geomagnetic data from the
51 past two decades [8], Figs 2a,d show that this trough connects two patches of
52 strong radial magnetic field at high latitude centred on Canada and Siberia. The
53 importance of these two patches in determining the structure of the field close to
54 the north magnetic pole has been well known for several centuries [14]. Both the
55 path of the north magnetic pole and the crucial Canadian and Siberian magnetic
56 patches are characteristics of the large-scale field [12], already evident when the
57 field is truncated at spherical harmonic degree $l=6$ (Figs 2b,e). Considered in iso-
58 lation from the remainder of the global field, each Earth-surface patch of strong
59 radial field would define a magnetic dip pole close to its centre point. The present
60 two-patch structure of the high latitude geomagnetic field then defines two ends

61 of a linear conduit of near vertical field along which the north magnetic pole can
62 readily travel.

63 Between 1999 and 2019, the Siberian patch showed a slight intensification
64 from a minimum value of -60.5 to $-60.6 \mu\text{T}$, while the Canadian patch decreased
65 significantly in absolute value from a minimum of -59.6 to $-58.0 \mu\text{T}$ (Fig 2a,d).
66 Together, these caused the direction of travel of the north magnetic pole to be
67 towards Siberia.

68 Although the magnetic field on Earth's surface is linearly related to the struc-
69 ture of the field on the core-mantle boundary (CMB), the geometric attenuation
70 through the mantle means that this relationship is not a simple mapping. For ex-
71 ample, the north magnetic pole does not correspond to a location on the CMB
72 where the horizontal field vanishes, but rather reflects a non-local averaging of
73 the field as shown in Figures 2b,c and 2e,f. The important Canadian and Siberian
74 surface patches are also spatial averages over regions dominated by the large-
75 scale lobes of intense magnetic flux underneath Canada and Siberia on the CMB
76 that are themselves fundamental features of the geodynamo process (Figs 2c,f)
77 [15]. We find that the time-dependent position of the pole along the conduit is
78 largely governed by a balance or tug-of-war between the competing influences
79 of the Canadian and Siberian lobes on the CMB. The angular offset between the
80 pole and these controlling flux lobes at mid to high latitudes ($50 - 70^\circ\text{N}$) is in ac-
81 cord with the relevant Green's functions for Laplace's equation under Neumann
82 boundary conditions [16; 17].

83 **Localised flux lobe elongation**

84 We now probe the physical mechanism that underpins the recent shift in balance
85 between the two flux lobes. Changes in the CMB radial magnetic field over 1999-
86 2019 (movie S1) show that the Canadian flux lobe (marked A, Fig 3c) elongated
87 longitudinally and divided into two smaller joined lobes (A' and B) within the
88 marked wedge (Fig 3a). Although lobe B has a higher intensity compared to lobe
89 A, importantly the spatial lengthscale of the magnetic field within the wedge has
90 decreased. The transfer of magnetic field from large to smaller scales caused the
91 weakening of the Canadian patch at Earth's surface because smaller scales attenu-
92 ate faster through the mantle with distance from the source. At the same time the
93 increasing proximity of lobe B to the Siberian lobe enhanced the Siberian surface
94 patch (Fig 3d). To demonstrate that this elongation effect is the primary cause of
95 the recent north magnetic pole movement, we performed a numerical experiment
96 where we isolated geomagnetic variation over the period 1999-2019 to within the

97 wedge (Figs 3a,c), the geomagnetic field being held fixed at its 1999 structure
98 elsewhere, and calculated the geomagnetic signature on the Earth's surface (see
99 methods). This simple model reproduces the weakening of the large-scale part of
100 the Canadian flux lobe at the CMB (Fig 3b) and the concomitant weakening of
101 the Canadian patch at Earth's surface (Fig 3d), in accord with Fig 2; it also repro-
102 duces the growth of the Siberian surface patch. Furthermore, it accounts for 961
103 km of the 1104 km (87%) distance travelled by the north magnetic pole over 1999-
104 2019. In a similar vein, we conducted additional numerical experiments (see figs
105 S1, S2 and methods) to test two other localised mechanisms previously proposed
106 to explain the recent north magnetic pole movement: those of intense geomag-
107 netic secular variation under the New Siberian Islands [16] and the influence of
108 a polar reversed-flux-patch on the CMB [11]. Both of these hypotheses produce
109 only small movements of the pole (travelling respectively 142 km and 16 km over
110 1999-2019). Prior to 1990, and at least as far back as 1940 (movie S2), the COV-
111 OBS.x1 geomagnetic model shows that the Canadian flux lobe was quasi-stable,
112 consistent with the slowly moving magnetic pole. In the 1990s, vigorous elonga-
113 tion leading up to the flux lobe splitting post 1999 resulted in the observed rapid
114 change in speed of the north magnetic pole.

115 **Interpretation in terms of core-flow**

116 Time variation of the geomagnetic field arises through a combination of core-flow
117 and magnetic diffusion. The reconfiguration of the Canadian flux lobe requires
118 a change in the signature in either or both of these two effects within the core
119 under Canada, although inference of any single underlying dynamical process is
120 non-unique. Here we base our interpretation on the frozen-flux assumption which
121 asserts that over decadal timescales the impact of core-flow is likely dominant
122 [18], and is consistent with the formation and advection of lobe B (Fig 3a). Fig
123 4a-c shows snapshots of the radial magnetic field with streamlines showing direc-
124 tion and magnitude of the large-scale core surface flow in 1970, 1999 and 2017,
125 depicting flow changes in this region during the acceleration phase of the north
126 magnetic pole. The presented flow models are the ensemble means of a series
127 of flows inferred by probabilistic inversions of both ground-based observatory
128 and satellite data, with a parameterisation of the unknown magnetic diffusion and
129 sub-grid scale induction processes [19; 20; 21]. In 1970, an intense large-scale
130 flow transported magnetic flux northwards under the east-coast of North Amer-
131 ica, connecting to a polar westwards flow around a section of the inner-core tan-
132 gent cylinder. Importantly, only a small part of the northward flow at that time

133 passed through the Canadian flux lobe. By 1999 the flow had altered into a broad
134 trans-North-America stream that converged and strengthened under Alaska: this
135 differential velocity was efficient at elongating (by stretching) the Canadian lobe
136 westwards. By 2017 the flow under Alaska had further strengthened, advection
137 and further stretching acting to separate the Canadian lobe into two pieces. Our
138 interpretation based on the presented ensemble mean flow is reinforced by the
139 fact that the basic sequence of events described above occurs in all flow ensemble
140 members.

141 The strengthening azimuthal flow under the Bering Straits, a key part of the
142 core-flow changes described above, may also be associated with the appearance
143 of an intense tangent-cylinder jet in this region, which has a clear observational
144 signature in the small-scale magnetic field (above spherical harmonic degree 11)
145 after 2004 [22]. However, such a tangent cylinder jet is in itself too localized
146 at high-latitude to be responsible for the elongation of the Canadian lobe in the
147 1990s that caused the rapid acceleration of the north magnetic pole. Instead it
148 seems that alteration in the global gyre structure [23; 24] beneath North America
149 began the elongation and contemporaneous north magnetic pole acceleration.

150 **Future predictions and historical perspectives**

151 Fig 1 shows a prediction of the future north magnetic pole position from a va-
152 riety of models: linear extrapolations from 2019 of the World Magnetic Model
153 (v2) [9] and CHAOS-6-x8 [8], and predictions based on the two end-member pro-
154 cesses generating geomagnetic secular variation, frozen-flux induction and pure
155 magnetic diffusion (see methods). All the models are based on recently observed
156 secular variation including the elongation of the Canadian flux lobe, and all pre-
157 dict a continuation of the current trajectory of the pole, with the greatest change
158 in position being from one flow ensemble member (660 km) and the minimum
159 change in position from the World Magnetic Model (v2) (390 km).

160 Will the north magnetic pole ever return to Canada? Given the delicate bal-
161 ance between the Canadian and Siberian flux lobes controlling the position of
162 the pole along the trough of weak horizontal field, it would take only a minor
163 readjustment of the present configuration to reverse the current trend. Predictions
164 of the magnetic field over decade to century timescales are on the horizon using
165 data assimilation methods [25; 26; 27], but these are still under development and
166 for now it is most informative to look at its past behaviour as a guide. Recon-
167 structions of the historical and archeomagnetic field over the past few thousand
168 years are inherently smoothed in time and based on sparse data, but nevertheless

169 can resolve the large-scale field patches that control the location of the magnetic
170 north pole. These reconstructions show that although the northern hemisphere has
171 largely been dominated by two flux patches, occasionally a three-patch structure
172 has arisen which would have had an effect on the pole's position [28; 29; 30].
173 Over the last 400 years, the pole has meandered quasi-stably around northern
174 Canada, but over the last 7000 years it seems to have chaotically moved around
175 the geographic pole, showing no preferred location [12]. Analogues of the recent
176 acceleration may have occurred at 4500 BC and 1300 BC when the speed reached
177 about 3-4 times the average seen in these reconstructions. The most recent of
178 these events coincided with the pole moving towards Siberia (from a region close
179 to Svalbard) where it remained stable for several hundred years. For now, a con-
180 clusive answer to the future location of the north magnetic pole will have to await
181 detailed monitoring of the geomagnetic field from the Earth's surface and space
182 in the coming years.

183 **Methods**

184 The isolation of geomagnetic secular variation in specific regions on the CMB
185 as shown in Figs 3, S1 and S2 is achieved using a physical grid: inside the
186 shown wedge the radial component of the geomagnetic field is allowed to evolve,
187 whereas outside it is frozen at its initial state. We transform to an equivalent
188 divergence-free magnetic-potential representation based on spherical harmonics,
189 which allows upward continuation of the magnetic field to the Earth’s surface. The
190 latitude-longitude grid has $L + 1$ Gauss-Legendre points in colatitude, and $3L + 1$
191 equally spaced points in longitude, where the maximum spherical harmonic de-
192 gree is $L = 13$. Note that any monopolar component or discontinuities caused
193 by adjoining two distinct magnetic field structures are removed by the projection
194 adopted.

195 To predict the north magnetic pole position using the large-scale flow ensem-
196 ble of [20; 21], for each ensemble member all spherical harmonic flow coefficients
197 are extrapolated 2019-2029 using a simple linear best fit through their values from
198 2014-2018. The rate of change of geomagnetic field is then computed from the
199 induction equation using the time-dependent large-scale flow along with a static
200 correction term. The geomagnetic field is then evolved through time using a first
201 order time-stepping scheme and the position of the north magnetic pole evaluated
202 using a descent method in the horizontal magnitude. The correction term is cho-
203 sen so that the Gauss coefficients (to degree 13) of the modelled rate of change of
204 geomagnetic field at 2019 match those from CHAOS-6-x8. Its static nature relies
205 upon on the assumption that both diffusion, and any small-small scale interactions
206 not captured in the large scale flow models, are time-independent over a 10-year
207 period. A purely-diffusive prediction is based on the model of [31], in which a
208 magnetic field diffuses from its initial state. The model is described by two ra-
209 dial basis functions for each poloidal spherical harmonic mode up to a maximum
210 spherical harmonic degree 13. The coefficients describing the initial field (here
211 taken to be in 2014) are chosen by fitting to CHAOS-6-x8 over the time period
212 2014-19. The model is then evolved beyond 2019 according to the diffusion equa-
213 tion; over this time period it differs from the linear extrapolation of CHAOS-6-x8.
214 Note that this procedure is not sensitive to the specific choice of time window: a
215 model fit over 2018-19 from an initial state in 2018 (not shown) is visually almost
216 indistinguishable from that fit over 2014-19.

217 **References**

- 218 [1] Ross, J. C. On the Position of the North Magnetic Pole. *Phil. Trans. R. Soc.*
219 *A* **124**, 47–52 (1834).
- 220 [2] Amundsen, R. *The Northwest Passage* (Archibald Constable & Co. Ltd,
221 London, 1908).
- 222 [3] Good, G. Follow the needle: seeking the magnetic poles. *Earth Sciences*
223 *History* **10**, 154–167 (1991).
- 224 [4] Newitt, L. R., Chulliat, A. & Orgeval, J.-J. Location of the North Magnetic
225 Pole in April 2007. *Earth, planets and space* **61**, 703–710 (2009).
- 226 [5] Thébaud, E. *et al.* International geomagnetic reference field: the twelfth
227 generation. *Earth, Planets and Space* **67** (2015).
- 228 [6] Friis-Christensen, E., Lühr, H. & Hulot, G. Swarm: A constellation to study
229 the Earth’s magnetic field. *Earth, planets and space* **58**, 351–358 (2006).
- 230 [7] Gillet, N., Barrois, O. & Finlay, C. C. Stochastic forecasting of the geomag-
231 netic field from the COV-OBS.x1 geomagnetic field model, and candidate
232 models for IGRF-12. *Earth Planets Space* **67**, 1321–14 (2015).
- 233 [8] Finlay, C. C., Olsen, N., Kotsiaros, S., Gillet, N. & Toffner-Clausen, L.
234 Recent geomagnetic secular variation from *Swarm* and ground observatories
235 as estimated in the CHAOS-6 geomagnetic field model. *Earth Planets Space*
236 **68**, 1–18 (2016).
- 237 [9] Chulliat, A. *et al.* Out-of-Cycle Update of the US/UK World Magnetic
238 Model for 2015-2020. Tech. Rep. (2019).
- 239 [10] Hope, E. R. Linear secular oscillation of the northern magnetic pole. *Journal*
240 *of Geophysical Research* **62**, 19–27 (1957).
- 241 [11] Olsen, N. & Manda, M. Will the magnetic North Pole move to Siberia?
242 *Eos, Transactions American Geophysical Union* **88**, 293–293 (2007).
- 243 [12] Korte, M. & Manda, M. Magnetic poles and dipole tilt variation over the
244 past decades to millennia. *Earth Planets Space* **60**, 937–948 (2008).

- 245 [13] Manda, M. & Dormy, E. Asymmetric behavior of magnetic dip poles. *Earth*
246 *Planets Space* **55**, 153–157 (2003).
- 247 [14] Hansteen, C. *Untersuchungen über den magnetismus der erde* (Christiania,
248 Gedruckt bey J. Lehmann und C. Gröndahl, 1819).
- 249 [15] Bloxham, J. & Gubbins, D. The secular variation of Earth’s magnetic field.
250 *Nature* **317**, 777–781 (1985).
- 251 [16] Chulliat, A., Hulot, G. & Newitt, L. R. Magnetic flux expulsion from the
252 core as a possible cause of the unusually large acceleration of the north mag-
253 netic pole during the 1990s. *J. Geophys. Res.* **115**, B07101 (2010).
- 254 [17] Gubbins, D. & Roberts, N. Use of the frozen flux approximation in the
255 interpretation of archaeomagnetic and palaeomagnetic data. *Geophys J. Int.*
256 **73**, 675–687 (1983).
- 257 [18] Roberts, P. H. & Scott, S. On analysis of secular variation. 1. A hydromag-
258 netic constraint - theory. *J Geomagn Geoelectr* **17**, 137–151 (1965).
- 259 [19] Barrois, O., Gillet, N. & Aubert, J. Contributions to the geomagnetic secular
260 variation from a reanalysis of core surface dynamics. *Geophysical Journal*
261 *International* **211**, 50–68 (2017).
- 262 [20] Barrois, O., Hammer, M. D., Finlay, C. C., Martin, Y. & Gillet, N. As-
263 similation of ground and satellite magnetic measurements: inference of core
264 surface magnetic and velocity field changes. *Geophys J. Int.* **215**, 695–712
265 (2018).
- 266 [21] Barrois, O. *et al.* Erratum: ‘Contributions to the geomagnetic secular varia-
267 tion from a reanalysis of core surface dynamics’ and ‘Assimilation of ground
268 and satellite magnetic measurements: inference of core surface magnetic and
269 velocity field changes’. *Geophys J. Int.* **216**, 2106–2113 (2018).
- 270 [22] Livermore, P. W., Hollerbach, R. & Finlay, C. C. An accelerating high-
271 latitude jet in Earth’s core. *Nature Geoscience* **10**, 62–68 (2017).
- 272 [23] Pais, A. & Jault, D. Quasi-geostrophic flows responsible for the secular
273 variation of the Earth’s magnetic field. *Geophys. J. Int.* **173**, 421–443 (2008).

- 274 [24] Gillet, N., Jault, D. & Finlay, C. C. Planetary gyre, time-dependent eddies,
275 torsional waves, and equatorial jets at the Earth's core surface. *J. Geophys.*
276 *Res.* **120**, 3991–4013 (2015).
- 277 [25] Aubert, J. Geomagnetic forecasts driven by thermal wind dynamics in the
278 earth's core. *Geophys J. Int.* **203**, 1738–1751 (2015).
- 279 [26] Tangborn, A. & Kuang, W. Impact of archeomagnetic field model data on
280 modern era geomagnetic forecasts. *Physics of the Earth and Planetary Inte-*
281 *riors* **276**, 2 – 9 (2018). Special Issue:15th SEDI conference.
- 282 [27] Sanchez, S., Wicht, J., Bärenzung, J. & Holschneider, M. Sequential as-
283 simulation of geomagnetic observations: perspectives for the reconstruction
284 and prediction of core dynamics. *Geophysical Journal International* **217**,
285 1434–1450 (2019).
- 286 [28] Nilsson, A., Holme, R., Korte, M., Suttie, N. & Hill, M. Reconstructing
287 Holocene geomagnetic field variation: new methods, models and implica-
288 tions. *Geophys J Int* **198**, 229–248 (2014).
- 289 [29] Constable, C., Korte, M. & Panovska, S. Persistent high paleosecular vari-
290 ation activity in southern hemisphere for at least 10 000 years. *Earth and*
291 *Planetary Science Letters* **453**, 78–86 (2016).
- 292 [30] Panovska, S., Constable, C. & Korte, M. Extending global continuous ge-
293 omagnetic field reconstructions on timescales beyond human civilization.
294 *Geochemistry, Geophysics, Geosystems* **19**, 4757–4772 (2018).
- 295 [31] Metman, M. C., Livermore, P. W., Mound, J. E. & Beggan, C. D. Modelling
296 decadal secular variation with only magnetic diffusion. *Geophysical Journal*
297 *International* **219**, S58–S82 (2019).

298 **Acknowledgements**

299 PWL acknowledges funding from the Natural Environment Research Council
300 (NERC) grant NE/P016758/1. CCF acknowledges funding the the European Re-
301 search Council (ERC) under the European Union's Horizon 2020 research and
302 innovation programme, grant agreement No. 772561.

303 **Data availability**

304 The CHAOS-6-x8 and COV-OBS.x1 geomagnetic field models on which this
305 study is based can be found at:

306 <http://www.spacecenter.dk/files/magnetic-models/>

307 The flow models of Barrois et al. employed here can be found at:

308 <https://geodyn.univ-grenoble-alpes.fr/>

309 **Code availability**

310 All codes are freely available by request from P.W. Livermore (email: p.w.livermore@leeds.ac.uk).

311 **Author contributions**

312 PWL and CCF devised the study; calculations were performed by PWL and MB.
313 CCF derived the CHAOS-6-x8 field model. PWL and CCF analysed the geomag-
314 netic field and core flow models, interpreted the results and wrote the paper. All
315 authors commented on the manuscript.

316 **Author information**

- 317 • The authors declare that they have no competing financial interests.
- 318 • Correspondence and requests for materials should be addressed to P.W. Liv-
319 ermore (email: p.w.livermore@leeds.ac.uk).

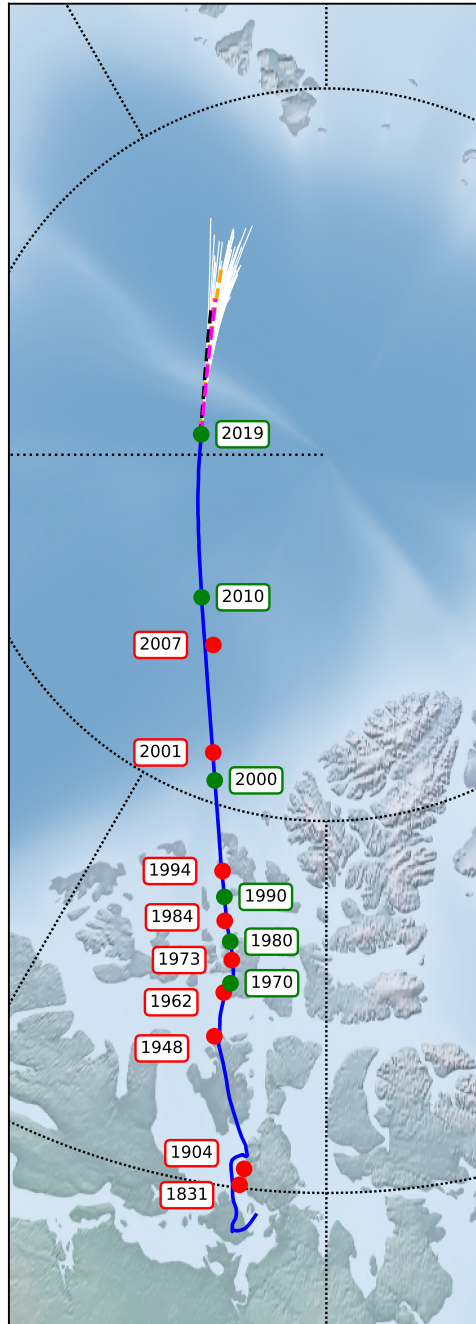


Figure 1: Historical movement and predicted future path of the North Magnetic pole in stereographic projection. Solid blue shows the pole's evolution according to the COV-OBS.x1 (1840-1998) and CHAOS-6-x8 (1999-2019) geomagnetic field models, with green circles indicating recent decadal positions; red circles mark in-situ measurements (1831-2007) [13; 4]. The international date line is shown by the dotted black line on the 180° meridian. Predictions (see methods) 2019-2029 are: linear extrapolation from the World Magnetic Model v2 [9] as black, linear extrapolation from CHAOS-6-x8 as magenta, a purely-diffusive model based on fitting geomagnetic secular variation over 2014-2019 in orange [31] and frozen-flux evolution using an ensemble of large-scale flows [20; 21] as white.

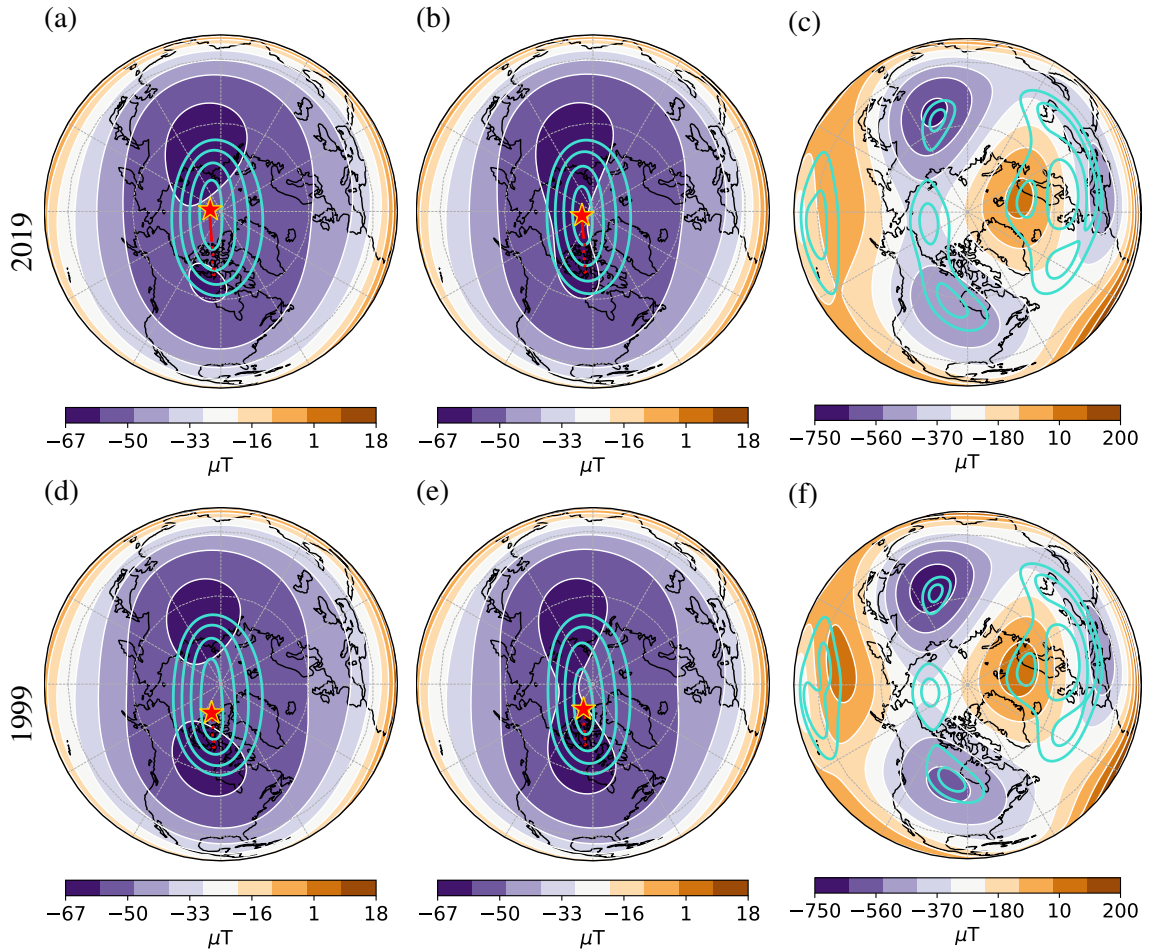


Figure 2: A comparison of the structure of the geomagnetic field and the north magnetic pole position in orthographic projection between 2019 (a-c) and 1999 (d-f). (a,d): contours of the radial field on the Earth's surface overlaid with contours of H in turquoise (values [2,4,6,8] μT) and the north magnetic pole as a red star with its dotted tail showing the path 1840-1999, solid tail 1999-2019. (b,e): as (a,d) but truncated to spherical harmonic degree 6. (c,f): structure of the geomagnetic field to degree 6 on the core-mantle-boundary, shown by contours of radial field overlaid with contours of H in turquoise (values [50,100] μT).

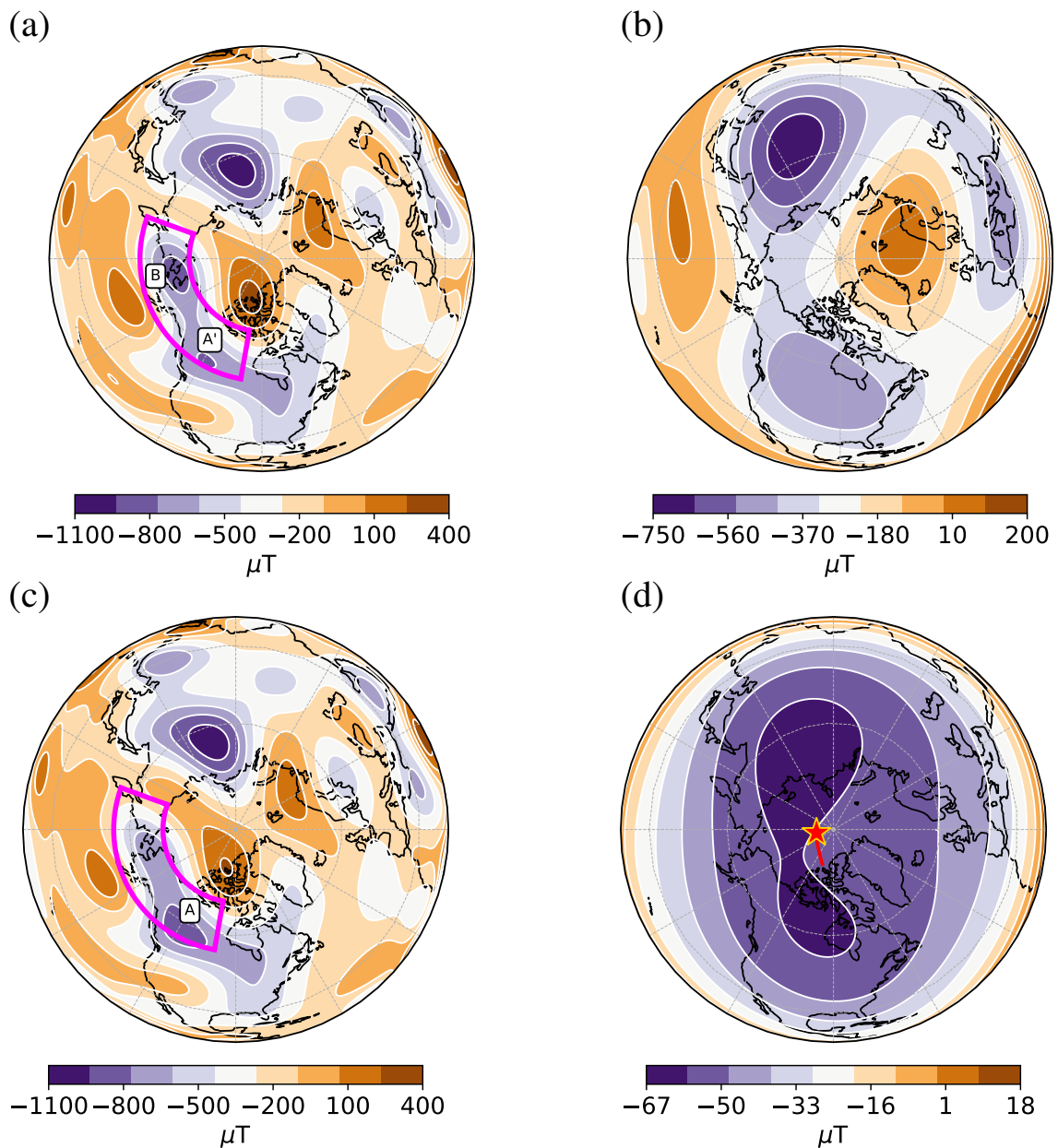


Figure 3: Experiment demonstrating the effect of elongation of the Canadian CMB flux lobe on the large-scale surface field and pole position. (c) contours of the radial component in 1999 according to CHAOS-6-x8. (a) radial component of a composite field projected into a divergence-free spherical-harmonic representation, comprising the structure in 2019 within the magenta wedge and the structure in 1999 elsewhere; (b) radial field on the CMB, as in (a) but truncated to degree 6, note the similar structure to Fig 2(c) demonstrates that flux lobe elongation explains the change in the Canadian surface patch; (d) radial field on the Earth's surface with the north magnetic pole (red star), whose tail indicates its path since 1999, produced only by changes within the wedge.

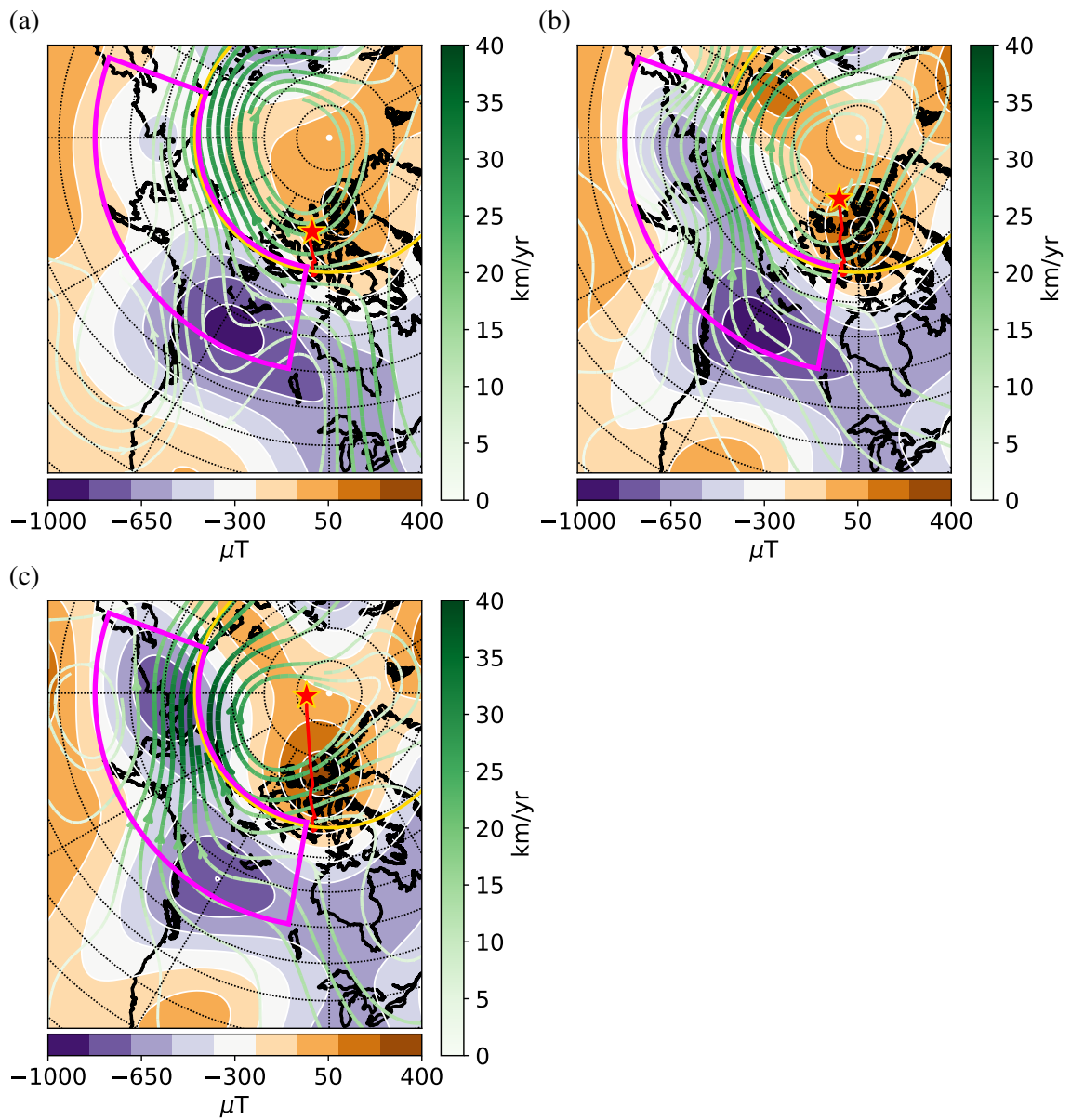


Figure 4: Local core surface dynamics around the Canadian flux lobe in stereographic projection. Shown are contours of the radial magnetic field, the north magnetic pole position and path since 1840, flow streamlines with arrows and the wedge within which flux lobe elongation occurs in (a) 1970, (b) 1999 and (c) 2017. The 1970 magnetic field and flow data is from COV-OBS.x1 and the ensemble mean flow of [19; 21]; those from 1999 are from CHAOS-6-x8 and the ensemble mean flow of [19; 21]; those from 2017 are from CHAOS-6-x8 and the ensemble mean of [20; 21]. The inner-tangent cylinder is marked in gold at about 69° N.